Title: A novel D-2-hydroxy acid dehydrogenase with high substrate preference for phenylpyruvate originating from lactic acid bacteria: structural analysis on the substrate specificity

Authors: Hoe-Suk Lee, Jisu Park, Young Je Yoo, Young Joo Yeon

PII: S0141-0229(19)30030-4
DOI: https://doi.org/10.1016/j.enzmictec.2019.02.008
Reference: EMT 9315

To appear in: *Enzyme and Microbial Technology*

Received date: 21 December 2018
Revised date: 15 February 2019
Accepted date: 22 February 2019

Please cite this article as: Lee H-Suk, Park J, Yoo YJ, Yeon YJ, A novel D-2-hydroxy acid dehydrogenase with high substrate preference for phenylpyruvate originating from lactic acid bacteria: structural analysis on the substrate specificity, *Enzyme and Microbial Technology* (2019), https://doi.org/10.1016/j.enzmictec.2019.02.008

A novel D-2-hydroxy acid dehydrogenase with high substrate preference for phenylpyruvate originating from lactic acid bacteria: structural analysis on the substrate specificity

Hoe-Suk Lee[a], Jisu Park[b], Young Je Yoo[a,c*], Young Joo Yeon[b*]

[a] *Program of Bioengineering, Seoul National University, 1 Gwanak-ro, Gwanak-gu, Seoul, 08826, Republic of Korea*

[b] *Department of Biochemical Engineering, Gangneung-Wonju National University, 7, Jukheon-gil, Gangneung-si, Gangwon-do, 25457, Republic of Korea*

[c] *School of Chemical and Biological Engineering, Seoul National University, 1 Gwanak-ro, Gwanak-gu, Seoul, 08826, Republic of Korea*

*Corresponding authors

E-mail addresses: hsl0828@snu.ac.kr (HS. Lee), jspark@gwnu.ac.kr (J. Park), yjyoo@snu.ac.kr (YJ. Yoo), yjyeon@gwnu.ac.kr (YJ. Yeon)

Highlights

- A novel D-LDH with high substrate preference for phenylpyruvate (PPA) was discovered.
- The catalytic efficiency of D-LDH from *P. claussenii* with PPA was 1,348 (s^{-1} mM^{-1}).
- Biochemical, phylogenetic and structural analysis for the enzymes were investigated.
- Phenyl ring of PPA interacts hydrophobically with phenylalanine in the active site.
- Structural analysis provides new engineering possibilities for D-LDHs.

Abstract

2-Hydroxy acid dehydrogenases (2-HADHs) have been implicated in the synthesis of 2-hydroxy acids from 2-oxo acids that are used in wide areas of industry. D-lactate dehydrogenases (D-LDHs), a subfamily of 2-HADH, have been utilized to this purpose, yet they exhibited relatively low catalytic activity to the 2-oxo acids with large functional groups at C_3. In this report, four putative 2-HADHs from *Oenococcus oeni*, *Weissella confusa*,

Weissella koreensis and *Pediococcus claussenii* were examined for activity on phenylpyruvate (PPA), a substrate to 3-phenyllactic acid (PLA) with a C_3 phenyl group. The 2-HADH from *P. claussenii* was found to have the highest k_{cat}/K_m on PPA with 1348.03 s^{-1} mM^{-1} among the four enzymes with higher substrate preference for PPA than pyruvate. Sequential, structural and mutational analysis of the enzyme revealed that it belonged to the D-LDH family, and phenylalanine at the position 51 was the key residue for the PPA binding to the active site via hydrophobic interaction, whereas in the 2-HADHs from *O. oeni* and *W. confusa* the hydrophilic tyrosine undermined the interaction. Because phenyllactate is a potential precursor for pharmaceutical compounds, antibiotics and biopolymers, the enzyme could increase the efficiency of bio-production of valuable chemicals. This study suggests a structural basis for the high substrate preference of the 2-HADH, and further engineering possibilities to synthesize versatile 2-hydroxy acids.

Keywords

D-2-hydroxy acid dehydrogenase; Phenyllactic acid; Substrate specificity; Structural analysis

1. Introduction

D-2-hydroxy acids are versatile building block compounds used in pharmaceutical, cosmetic and organic synthetic industries, including D-2-hydroxybutanoate, D-2-hydroxy-4-phenylbutyrate and D-phenyllactic acid (D-2-hydroxy-3-phenylpropanoic acid, D-PLA) [1-4]. Recently, special attention has been focused on the synthesis of D-PLA for its antimicrobial activity against various deleterious bacteria and fungi [5-9] as well as a precursor to Danshensu (3,4-dihydroxyphenyllactic acid), a drug for cardiovascular diseases [10]. Potent uses as a monomeric substrate of poly(PLA) has also been reported [11]. D-PLA was discovered as a metabolite of lactic acid bacteria (LAB) [6, 12], and many D-lactate dehydrogenase (D-LDH, EC. 1.1.1.28) genes were cloned from various species of LAB strains for the synthesis of D-PLA from phenylpyruvate (PPA) [4, 9, 13-18]. D-

lactate dehydrogenase is a member of D-isomer-specific 2-hydroxy acid dehydrogenase (D-2-HADH) family with typical two Rossmann-fold motifs each constituting a catalytic domain and a cofactor binding domain [19-23]. Many structural studies with pyruvate, the primary substrate, show that D-LDHs are allosteric dimers with the active site located in the interface of the two domains [19, 21]. The cofactor binding domain side of the active site comprises of a bound NADH and a H296 whose pKa is modified by E264, for a hydride transfer to the pyruvate C_2 and 2-oxo group, respectively [19, 21, 22, 24]. R235 is known to stabilize the carboxylic group of pyruvate from face-on or at an angle. N77, V78 and G79 from the catalytic domain side of the active site were also proposed to stabilize the carboxylic group in a productive binding mode. Cofactor and substrate binding enables a motion of the two domains so that pyruvate is tightly held by the residues from both side. However, much less is known for the PPA binding to these D-LDHs compared to the detailed structural analysis with respect to pyruvate.

In this study, four putative 2-hydroxy acid dehydrogenases (2-HADH) based on the homologous amino acid sequences in four LAB species, *Oenococcus oeni*, *Weissella confusa*, *Weissella koreensis*, and *Pediococcus claussenii* (oo, wc, wk and pcHADH, henceforth), were examined for the enzymatic synthesis of D-PLA from PPA. Phylogenetic analysis indicated oo, wc and pcHADH belong to the D-LDH subfamily, while wkHADH is a member of glyoxylate-hydroxypyruvate subfamily of the D-2-HADH family. A wild-type enzyme that belongs to the D-LDH family but with higher substrate specificity for PPA than pyruvate was found, whereas wild-types of other members of this family generally display pyruvate preference, although several engineering attempts succeeded in creating PPA-specific enzymes [4, 13, 25, 26]. Structural analysis with PPA bound to the active site of the enzymes was carried out to explain their substrate specificities. The enzyme with higher preference for PPA and its structural analysis will help developing biocatalysts capable of synthesizing α-2-hydroxy acid with larger substituent (phenyl, 4-hydroxyphenyl or aliphatic chains with a length of 4 ~ 6 carbon) at C_3 position.

2. Materials & methods

2.1 Materials

The ooHADH, wcHADH, wkHADH and pcHADH genes were synthesized from GenScript (New Jersey, USA)

with additional C-terminal His_6-tag and codon optimization for *E. coli* [27, 28]. Their NCBI accession numbers are as follows; ooHADH (MH920337), wcHADH (MH920336), wkHADH (MH920338) and pcHADH (MH920335). They were cloned in pET22b(+) vectors using NdeI and XhoI restriction sites. Oligonucleotide synthesis and mutation sequencing were performed by Cosmogenetech (Seoul, Korea). *E. coli* strains were purchased from Invitrogen (Carlsbad, CA). Sodium phenylpyruvate was purchased from Tokyo Chemical Industry (Tokyo, Japan). All other chemicals were purchased from Sigma-Aldrich (St Louis, USA).

2.2 Mutagenesis, expression and purification of 2-HADHs

The 2-HADH genes were transformed into *E. coli* DH5α for cloning and mutation and *E. coli* BL21 (DE3) for expression. The pcHADH gene was mutated with the primers described in the Supplemental material S1 following the QuikChange II Site-Directed Mutagenesis protocol (Agilent, Santa Clara, USA). The cells transformed with wild-type ooHADH, wcHADH, wkHADH, pcHADH and mutant pcHADH were grown for 16 h in lysogeny broth (LB) medium supplemented with 100 μg/ml ampicillin, at 37 °C and 200 rpm under aerobic conditions. For protein expression purposes, 50 ml of BL21 cell culture were grown to reach the optical density at 600 nm (OD_{600}) of 0.6, followed by induction with 0.8 mM isopropyl β-D-1-thiogalactopyranoside (IPTG) at 20 °C, 200 rpm for 24 h. The induced cell cultures were harvested by centrifugation at 3200 rpm, 4 °C for 20 minutes. Harvested cells were lysed by Bugbuster® (Merck Millipore, Billerica, USA), centrifuged (8000 rpm, 4 °C, 20 min) for cell debris removal and subjected to Ni-affinity chromatography (Qiagen, Hilden, Germany) for elution with 250 mM imidazole. Purification of the enzymes to homogeneity was confirmed by SDS-PAGE. Protein concentration was determined by the Bradford method using bovine serum albumin as a standard [13, 29].

2.3 Enzyme activity assays with the purified 2-HADHs

In vitro enzyme activity was assayed at 30 °C in 1ml cuvette containing 50 mM sodium acetate buffer (pH 5.5), 0.2 mM NADH, up to 20 mM pyruvate or PPA as a substrate, and 0.5-5.4 μg of the purified enzyme. The rate of NADH decrease was determined by absorbance change at 340 nm, with molar extinction coefficient of 6.22 $mM^{-1}cm^{-1}$ in a spectrophotometer (Molecular Devices, San Jose, USA). One unit of enzyme activity was defined as the amount of enzyme that oxidizes 1 μmol NADH per minute. The specific enzyme activity was measured as

units per milligram of protein [14]. Apparent k_{cat} and K_m were calculated by measuring activities on varying degree of substrate concentrations (0.04 ~ 40 mM) and fitting the data to the Michaelis-Menten equation. All measurements were carried out in triplicates.

2.4 *In vitro* enzymatic conversion of PPA into PLA

Conversion of PPA into PLA was analyzed via HPLC. The reaction mixture consisted of 8.59 nM purified 2-HADH, 20 mM PPA, 1.5 mM NADH, 30 mM sodium formate, 1 unit of formate dehydrogenase from *Candida boidinii* (Sigma Aldrich, St Louis, USA) and 50 mM sodium acetate buffer (pH 6.5) in total volume of 3 ml. The mixture was sampled at 0, 0.5, 1, 2, 4, 8 and 12 h, heat-inactivated at 99 °C, centrifuged for 5 min (13000 rpm), and filtered by 0.2 μm Whatman PVDF filter (GE Healthcare, Pittsburgh, USA) before being subjected into YL9100 HPLC system (YL instruments, Anyang, Korea) installed with Aminex® HPX-87H Ion exclusion Column (300 mm x 7.8 mm) from Bio-Rad (Hercules, USA). 5 mM H_2SO_4 was used as a mobile phase at a flow rate of 0.6 ml min^{-1} and the peaks for PPA and PLA were observed at 19.42 min and 41.28 min respectively, at 37 °C by a UV detector at 210 nm [26]. For a chiral detection of the enantiomeric PLA product, Chiralcel OJ-H column (250 mm x 0.46mm, 5 μm) from Daicel (Tokyo, Japan) was used with a mobile phase of hexane, 2-propanol, and trifluoroacetic acid in 90:10:0.1 (v:v), and UV detection at 261 nm. PPA was detected at 38 min, D-PLA at 30 min and L-PLA at 34 min.

2.5 Phylogenetic analysis and multiple sequence alignment

Phylogenetic trees were constructed using the four 2-HADHs and seven other D-LDHs previously reported to have PPA reductase activity, along with 365 sequences that belong to the D-2-HADH family. The D-LDH sequences from following species were retrieved from NCBI database, with their accession numbers in parenthesis: *P. pentosaceus* ATCC25745 D-LDH (CP000422), *P. acidilactici* DSM20284 D-LDH (X70925), *L. plantarum* SK002 D-LDH (FJ712707), *L. pentosus* JCM1558 D-LDH (P26298), *B. coagulans* SDM D-LDH (HQ148710), *L. bulgaricus* ATCC11842 D-LDH (CR954253) and *S. inulinus* CASD (MG579976). All other sequences were obtained from PROSITE database (ID: PDOC00063) [30]. A neighbor-joining unrooted tree was generated with MEGA-X 10.0.5 software using 100 iterations and a 60% threshold value for bootstraps [31,

32]. Multiple sequence alignment was carried out using Clustal Omega [33].

2.6 Homology modeling and molecular docking

Homology models of ooHADH, wcHADH and pcHADH were constructed based on the X-ray crystal structures of D-lactate dehydrogenase from *Lactobacillus helveticus* and *Lactobacillus bulgaricus* (PDB: 2dld and 1j49 respectively) [21]. The templates were determined by searching each sequence against the Protein Data Bank database using the position specific iterated-BLAST algorithm [34, 35]. The secondary structures were aligned between the templates and the query sequences and homology modeling was carried out by the Prime homology modeling program from Schrödinger [36]. The crystal-bound NAD was manually changed to NADH and energy minimized. The stereochemical quality of the models were validated by Ramachandran Plot in Rampage server [37]. Glide program from Schrödinger was used for the docking of the substrate into the homology modeled structures with OPLS3 forcefield [38, 39]. The grid-generation module from Glide was used to generate grids comprising the active sites of the 2-HADHs and the nicotinamide group of NADH. Pyruvate and PPA as ligands were created with all possible ionization states via LigPrep [40]. Standard Precision mode of Glide was used to produce docking poses.

3. Results & discussion

3.1 Activity screening of 2-HADHs

The four 2-HADHs were heterologously expressed in *E. coli* BL21 (DE3) and purified up to 5 mg, and their *in vitro* enzymatic activities toward pyruvate and PPA were determined (Fig. 1). For pyruvate, wcHADH showed the highest activity with 428 U mg^{-1}. pcHADH and ooHADH had 0.67 and 0.55 fold lower activities than the wcHADH, respectively. For PPA, however, pcHADH was found with the highest activity of 591 U mg^{-1}. Activities of ooHADH and wcHADH were much lower than pcHADH, 0.03 and 0.15 fold respectively. wkHADH had no significant activities against either pyruvate or PPA, even though Bradford assay showed all four 2-HADHs were expressed in similar quantities.

3.2 Kinetic parameters of 2-HADHs

The kinetic parameters of the 2-HADHs for pyruvate and PPA were determined using NADH as the cofactor (Table 1). Apparent $K_{m\ (PPA)}$ was 14 ~ 16 fold higher than $K_{m\ (pyruvate)}$ in ooHADH and wcHADH, indicating low binding affinity with PPA in these enzymes. On the other hand, pcHADH maintained low K_m for both pyruvate and PPA, notably slightly lower $K_{m\ (PPA)}$. In terms of $k_{cat\ (pyruvate)}$, wcHADH showed 2 ~ 3 fold higher value than oo and pcHADH. $k_{cat\ (PPA)}$ was the highest with pcHADH, closely followed by wcHADH, which were 6 fold higher than that of ooHADH. The overall catalytic efficiency, $k_{cat\ (pyruvate)}/K_{m\ (pyruvate)}$, was the highest with wcHADH (1124 s^{-1} mM^{-1}), and $k_{cat\ (PPA)}/K_{m\ (PPA)}$ was the highest with pcHADH (1348 s^{-1} mM^{-1}). This suggests pcHADH as a promising biocatalyst for biosynthesis of D-PLA, as it shows an inversion of substrate specificity for PPA over pyruvate, unlike many other D-LDH wild-types from previous studies (Table 2).

In addition, enzymatic conversion of PPA into PLA was confirmed by HPLC analysis of *in vitro* batch reaction with 20 mM of PPA (Fig. 2). In correlation with the kinetic parameters, the pcHADH was able to convert over 80 % of the PPA within 2 h, with productivity of 1.4 g^{-1} L^{-1} hr^{-1}. The oo and wcHADH did not reach 100 % conversion within the timescale of the experiment. Chiral column HPLC detected the peaks for the D-isomer but no L-isomer of PLA in the reaction by oo, wc and pcHADH. Unreacted remnant of PPA was also detected in the reaction by oo and wcHADH (Supplemental material S2).

3.3 Phylogenetic analysis and sequence alignment

A phylogenetic analysis on the 2-HADHs examined in this study as well as 365 members of D-2-HADH family with non-redundant sequences revealed the ooHADH, wcHADH and pcHADH belonged to the D-LDH subfamily, whereas wkHADH belonged to D-3-phosphoglycerate dehydrogenase subfamily which may explain its negligible activity with the pyruvate or PPA (Fig. 3a). All four 2-HADHs had a conserved sequence of G-X-G-X-X-G (where X represents any of the 20 amino acids) for a dinucleotide binding motif at the position 151 ~ 163, similar to the D-2-HADHs characteristic described by Taguchi and Ohta, compared to L-isomer specific 2-HADHs with the same motif at the position 28-33 [23]. Furthermore, ooHADH, wcHADH and pcHADH had Y174 or equivalent that was found to be crucial for NADH-dependency over NADPH, as reported by Zhu et al., in the study of $NADP^+$ preferred D-LDH from *S. inulinus* [41].

The four 2-HADHs and seven D-LDHs previously reported to have PPA reductive activity were further

analyzed for phylogenetic relationship (Fig. 3b). The sequence of pcHADH revealed a close relationship with *P. acidilactici* DSM 20284 D-LDH and *P. pentosaceus* D-LDH, while the ooHADH and the wcHADH were closer to *L. bulgaricus* ATCC 11842 D-LDH. Both D-LDHs from *P. acidilactici* DSM 20284 and *P. pentosaceus* have presented relatively high catalytic efficiencies of 105 and 100 s^{-1} mM^{-1} for PPA [9, 14]. However, it is notable that D-LDHs from *P. acidilactici* and *P, pentosaceus* have substrate specificity for pyruvate over PPA, yet pcHADH with a closely related sequence have inverted substrate preference. *L. bulgaricus* ATCC 11842 D-LDH had only k_{cat}/K_m of 1.0 s^{-1} mM^{-1} [4], showing similar catalytic efficiency with ooHADH and wcHADH.

Multiple sequence alignment via Clustal Omega shows highly conserved residues in the active site including the R234, N76, V77 and G78 known to stabilize the carboxylate and 2-oxo functional groups of the substrates via hydrogen bonding, H295 as a proton donor for reduction of the oxo group, and E263 modulating the pKa of the H295 (Fig. 4, corresponding residues are numbered based on those of pcHADH henceforth) [21]. In *B. coagulans* D-LDH and *S. inulinus* D-LDH several different amino acid residues at the position 51, 76-77, 100, 105 and 298 in the active site may have led to their comparatively low k_{cat}/K_m of 3.9 and 1.49 s^{-1} mM^{-1}, respectively [13, 16]. Notably, the pcHADH with the highest $k_{cat\ (PPA)}/K_{m\ (PPA)}$ among wild-type D-LDHs has the same residues in the active site, but with phenylalanine at the position 51 instead of tyrosine such as most other D-LDHs. The corresponding position has been recognized as a recognition site for the side chain of 2-oxo acids and subjected to engineering in many D-LDHs [4, 13, 25, 26, 42].

3.4 Mutation study of pcHADH

The pcHADH was subjected to mutation to examine the effect of the F51 on its activity. The position was mutated into aliphatic residues or aromatic residues as well as hydrophilic serine for variance in steric size and hydrophobicity. The wild-type pcHADH had the highest specific activity for PPA of 611 U mg^{-1} followed by 95 % relative activity with F51G mutation, but mostly with much lower activities (Fig. 5). Furthermore, mutation of F51 into tyrosine as in most wild-types of D-LDHs decreased up to 4% relative activity on phenylpyruvate, but retained 99% relative activity on pyruvate (data not shown). Mutation into leucine that had predominant activity improvement from previous studies in *L. pentosus* and *L. bulgaricus* D-LDH decreased relative activity to 10% [4, 25, 26, 42]. In these studies, mutations into aliphatic residues such as leucine, alanine and valine were carried out based on the work of Tokuda et al., where a sequence alignment of D-LDHs with *L. casei* D-

hydroxyisocaproate dehydrogenase revealed a possibility of leucine to accommodate 2-oxo acid substrates with larger C_3 substituents [42]. From our work, phenyalanine at the position 51 is a plausible mutation candidate for a high PPA activity, including but not limiting to pcHADH considering the similarities in the folds and the active site structures of many D-2-HADHs and D-LDHs [23, 43].

3.5 Structural analysis of the 2-HADHs

For structural modeling of oo, wc and pcHADHs that showed the activities toward both pyruvate and PPA, they were homology modeled based on structural templates from D-LDHs of *L. helveticus* (PDB: 2dld) and *L. bulgaricus* (PDB: 1j49) which showed the highest sequence identity (ooHADH, 69%; wcHADH, 68%; pcHADH, 50%). The validity of the homology models was confirmed by the Rampage server, which provided Ramachandran plot data for ooHADH, wcHADH and pcHADH as 96.4%, 97.0% and 99.1% of the residues in favored/allowed region, respectively. This is comparable to the 95.8% for 2dld and 99.5% for 1j49 whose structures are from X-ray crystallography.

Pyruvate and PPA were then docked as a substrate in the active site of the 2-HADHs to explain the activity (Fig. 6). Productive binding modes of the substrates are in reference to the oxamate analog in 2dld, and the configuration of pyruvate modeled in the active site of 1j49 [21]. The three 2-HADHs revealed a similar active site environment, except F51 for pcHADH, yet there were deviations to the binding of the substrates in all three enzymes. In oo and pcHADH, the carboxylate groups of the pyruvate and PPA were stabilized by hydrogen bonding with the N76-V77-G78 backbone and Y100 side chain in the catalytic domain. In wcHADH, PPA followed similar configuration, but pyruvate was rotated for the carboxylate to face stabilization by R235, which may account for its high pyruvate activity. Both mechanisms had been proposed previously where these configurations were regarded to enable the required electron transfer from the donors, NADH and H295, to substrates for reductive catalysis [21].

The hydride transfer distances between the NADH and the C_2 of the substrate (d1) and between H295 and substrate 2-oxo group (d2), which affect the activation free energy barrier are presented in Table 3 [44]. For PPA, pcHADH showed $d1_{(PPA)}$ and $d2_{(PPA)}$ values of 4.1 Å and 3.3 Å. The wcHADH with similar $k_{cat\ (PPA)}$ as pcHADH presented increased $d1_{(PPA)}$ but decreased $d2_{(PPA)}$ (5.7 Å and 2.7 Å), while the ooHADH with 6 fold reduced

$k_{cat(PPA)}$ had similar $d2_{(PPA)}$ as pcHADH but longer $d1_{(PPA)}$ (6.3 Å). The pcHADH had similar $k_{cat\ (pyruvate)}$ as $k_{cat\ (PPA)}$, in correlation with longer $d1_{(pyruvate)}$ (5.1 Å) but shorter $d2_{(pyruvate)}$ (2.8 Å) than those for PPA.

In order to see the effect of residue 51 on the substrate recognition, the distances from the centroid of the phenyl substituent of PPA or C_3 of pyruvate to the centroid of the phenyl ring of the residue 51 (d3) as well as to the hydroxyl group of tyrosine in oo and wcHADH (d4) were measured. The $d3_{(PPA)}$ and $d4_{(PPA)}$ showed that pcHADH (4.2 Å) had a stable hydrophobic contact with the phenyl substituent while in oo and wcHADH the residue was farther away from the substituent (7.4 Å for d3 and 6.1 ~7.0 Å for d4), an indication of relatively unfavorable interaction with the hydrophilic tyrosine. It was shown that the phenyl substituent is steered by the tyrosine in oo and wcHADH, distorting the binding form of PPA so that the d1 becomes larger in the Fig. 6. Steric hindrance effect is also expected due to the additional hydroxyl groups in the tyrosine. For pyruvate, the tyrosine has less steric and hydrophilic effect on the small C_3, whereas hydrophobic phenylalanine in pcHADH could be drawing the C_3, resulting in longer $d1_{(pyruvate)}$ and lower $k_{cat(pyruvate)}$ than those for PPA.

In terms of binding free energy, more stable binding of PPA marked by $\Delta G_{binding(PPA)}$ were in line with lower apparent K_m. $\Delta G_{binding(pyruvate)}$ showed similar values for all three enzymes, with respect to similar apparent K_m. However, there is no correlation between ΔG of pyruvate and PPA with respect to K_m, because the large phenyl group of PPA contributes more in the binding energy calculation as indicated by 2 fold lower $\Delta G_{binding(PPA)}$ than $\Delta G_{binding(pyruvate)}$.

Modeling of PPA with pcHADH mutants was also carried out to examine the mutation effect (Fig. 7 and Table 4). The carboxylate group of PPA was directed away from the N76-V77-G78 loop in F51L mutant, marked by the longer distance to the backbone nitrogen of G78 residue (d6). The d1 increased, as opposed to d2 in F51L in comparison to the wild-type. The $\Delta G_{binding(PPA)}$ indicated less binding affinity in the mutants, which could be due to less hydrophobic effect exerted by a longer distance to the leucine than phenylalanine. The pcHADH F51G and F51S mutants, which are expected to have less hydrophobic effect than F51L due to the longer d3, were more stabilized by the shorter d6 than the F51L mutant in correlation with their rather high relative specific activities.

4. Conclusion

Screening of dehydrogenases capable of synthesizing versatile 2-hydroxy acids is important for industrial applications. Many previous studies have reported enzymes to improve the activity on PPA, with focuses on Y52L in various D-LDHs. In this study, four putative 2-HADHs were investigated for the PPA activity, of which pcHADH presented the highest catalytic efficiency and more substrate preference for PPA than pyruvate. Phylogenetic analysis revealed it belonged to a D-LDH family, and a detailed structural analysis of the active site with both reducing cofactor and PPA brought phenylalanine residue at the position 51 of pcHADH to attention. Phenylalanine at the position was not engineered in other D-LDHs previously to our knowledge, and it seems to make a strong hydrophobic interaction with PPA in pcHADH. Further engineering possibilities on other D-LDHs and 2-HADHs based on our structural analysis are open for synthesis of 2-hydroxy acids with large functional substituents at C_3.

Conflict of interest statement

The authors declare that there are no conflicts of interest.

Acknowledgement

This research was supported by the Technology Development Program to Solve Climate Changes of the National Research Foundation (NRF) funded by the Ministry of Science and ICT (Grant Number: 2017M1A2A2087630).

Appendix A. Supplementary Material

The following is supplementary data to this article:

References

[1] K. Miltenberger, Hydroxycarboxylic Acids, Aliphatic, Ullmann's Encyclopedia of Industrial Chemistry, Wiley-VCH Verlag GmbH & Co. KGaA, Gersthofen, 2012. https://doi.org/10.1002/14356007.a13_507.

[2] B. Chen, H.F. Yin, Z.S. Wang, J.Y. Liu, J.H. Xu, A new chemo-enzymatic route to chiral 2-hydroxy-4-phenylbutyrates by combining lactonase-mediated resolution with hydrogenation over Pd/C, Chem Commun (Camb) 46(16) (2010) 2754-2756. https://doi.org/10.1039/b925402a.

[3] C. Gao, W. Zhang, C. Ma, P. Liu, P. Xu, Kinetic resolution of 2-hydroxybutanoate racemic mixtures by NAD-independent L-lactate dehydrogenase, Bioresour Technol 102(7) (2011) 4595-4599. https://doi.org/10.1016/j.biortech.2011.01.003.

[4] Z. Zheng, B. Sheng, C. Gao, H. Zhang, T. Qin, C. Ma, P. Xu, Highly stereoselective biosynthesis of (R)-alpha-hydroxy carboxylic acids through rationally re-designed mutation of D-lactate dehydrogenase, Sci Rep 3 (2013) 3401. https://doi.org/10.1038/srep03401.

[5] W. Mu, S. Yu, L. Zhu, T. Zhang, B. Jiang, Recent research on 3-phenyllactic acid, a broad-spectrum antimicrobial compound, Appl Microbiol Biotechnol 95(5) (2012) 1155-1163. https://doi.org/10.1007/s00253-012-4269-8.

[6] P. Lavermicocca, F. Valerio, A. Evidente, S. Lazzaroni, A. Corsetti, M. Gobbetti, Purification and characterization of novel antifungal compounds from the sourdough *Lactobacillus plantarum* strain 21B, Appl Environ Microbiol 66(9) (2000) 4084-4090. https://doi.org/10.1128/AEM.66.9.4084-4090.2000.

[7] S.M. Schwenninger, C. Lacroix, S. Truttmann, C. Jans, C. Sporndli, L. Bigler, L. Meile, Characterization of low-molecular-weight antiyeast metabolites produced by a food-protective *Lactobacillus-Propioni* bacterium coculture, J Food Prot 71(12) (2008) 2481-2487. https://doi.org/10.4315/0362-028X-71.12.2481.

[8] F. Valerio, M. Favilla, P. De Bellis, A. Sisto, S. de Candia, P. Lavermicocca, Antifungal activity of strains of lactic acid bacteria isolated from a semolina ecosystem against *Penicillium roqueforti*, *Aspergillus niger* and *Endomyces fibuliger* contaminating bakery products, Syst Appl Microbiol 32(6) (2009) 438-448. https://doi.org/10.1016/j.syapm.2009.01.004.

[9] S. Yu, H. Jiang, B. Jiang, W. Mu, Characterization of D-lactate dehydrogenase producing D-3-phenyllactic acid from *Pediococcus pentosaceus*, Biosci Biotechnol Biochem 76(4) (2012) 853-855. https://doi.org/10.1271/bbb.110955.

[10] L. Zhou, Z. Zuo, M.S. Chow, Danshen: an overview of its chemistry, pharmacology, pharmacokinetics, and clinical use, J Clin Pharmacol 45(12) (2005) 1345-1359. https://doi.org/10.1177/0091270005282630.

[11] H.D. Nguyen, X. Jin, D. Kaneko, T. Kaneko, Syntheses of high molecular weight poly(L-phenyllactic acid)s by a direct polycondensation in the presence of stable lewis acids, Chemistry Letters 40(6) (2011) 584-585. https://doi.org/10.1246/cl.2011.584.

[12] K. Strom, J. Sjogren, A. Broberg, J. Schnurer, *Lactobacillus plantarum* MiLAB 393 produces the antifungal cyclic dipeptides cyclo(L-Phe-L-Pro) and cyclo(L-Phe-trans-4-OH-L-Pro) and 3-phenyllactic acid, Appl Environ Microbiol 68(9) (2002) 4322-4327. https://doi.org/10.1128/AEM.68.9.4322-4327.2002.

[13] M. Wang, L. Zhu, X. Xu, L. Wang, R. Yin, B. Yu, Efficient production of enantiomerically pure D-phenyllactate from phenylpyruvate by structure-guided design of an engineered D-lactate dehydrogenase, Appl Microbiol Biotechnol 100(17) (2016) 7471-7478. https://doi.org/10.1007/s00253-016-7456-1.

[14] W. Mu, S. Yu, B. Jiang, X. Li, Characterization of D-lactate dehydrogenase from *Pediococcus acidilactici* that converts phenylpyruvic acid into phenyllactic acid, Biotechnol Lett 34(5) (2012) 907-911. https://doi.org/10.1007/s10529-012-0847-1.

[15] J. Jia, W. Mu, T. Zhang, B. Jiang, Bioconversion of phenylpyruvate to phenyllactate: gene cloning, expression, and enzymatic characterization of D- and L1-lactate dehydrogenases from *Lactobacillus plantarum* SK002, Appl Biochem Biotechnol 162(1) (2010) 242-251. https://doi.org/10.1007/s12010-009-8767-9.

[16] Z. Zheng, C. Ma, C. Gao, F. Li, J. Qin, H. Zhang, K. Wang, P. Xu, Efficient conversion of phenylpyruvic acid to phenyllactic acid by using whole cells of *Bacillus coagulans* SDM, PLoS One 6(4) (2011) e19030. https://doi.org/10.1371/journal.pone.0019030.

[17] L. Chen, Y. Bai, T.P. Fan, X. Zheng, Y. Cai, Characterization of a D-lactate dehydrogenase from *Lactobacillus fermentum* JN248 with high phenylpyruvate reductive activity, J Food Sci 82(10) (2017) 2269-2275. https://doi.org/10.1111/1750-3841.13863.

[18] G.C. Xu, L.L. Zhang, Y. Ni, Enzymatic preparation of D-phenyllactic acid at high space-time yield with a novel phenylpyruvate reductase identified from Lactobacillus sp. CGMCC 9967, J Biotechnol 222 (2016) 29-37. https://doi.org/10.1016/j.jbiotec.2015.12.011.

[19] S.V. Antonyuk, R.W. Strange, M.J. Ellis, Y. Bessho, S. Kuramitsu, Y. Inoue, S. Yokoyama, S.S. Hasnain, Structure of D-lactate dehydrogenase from *Aquifex aeolicus* complexed with NAD(+) and lactic acid (or

pyruvate), Acta Crystallogr Sect F Struct Biol Cryst Commun 65(Pt 12) (2009) 1209-1213. https://doi.org/10.1107/S1744309109044935.

[20] A.S. Kutzenko, V.S. Lamzin, V.O. Popov, Conserved supersecondary structural motif in NAD-dependent dehydrogenases, FEBS Lett 423(1) (1998) 105-109. https://doi.org/S0014-5793(98)00074-X.

[21] A. Razeto, S. Kochhar, H. Hottinger, M. Dauter, K.S. Wilson, V.S. Lamzin, Domain closure, substrate specificity and catalysis of D-lactate dehydrogenase from *Lactobacillus bulgaricus*, J Mol Biol 318(1) (2002) 109-119. https://doi.org/10.1016/S0022-2836(02)00086-4.

[22] T. Shinoda, K. Arai, M. Shigematsu-Iida, Y. Ishikura, S. Tanaka, T. Yamada, M.S. Kimber, E.F. Pai, S. Fushinobu, H. Taguchi, Distinct conformation-mediated functions of an active site loop in the catalytic reactions of NAD-dependent D-lactate dehydrogenase and formate dehydrogenase, J Biol Chem 280(17) (2005) 17068-17075. https://doi.org/10.1074/jbc.M500970200.

[23] H. Taguchi, T. Ohta, D-lactate dehydrogenase is a member of the D-isomer-specific 2-hydroxyacid dehydrogenase family. Cloning, sequencing, and expression in *Escherichia coli* of the D-lactate dehydrogenase gene of *Lactobacillus plantarum*, J Biol Chem 266(19) (1991) 12588-12594.

[24] S. Kochhar, N. Chuard, H. Hottinger, Glutamate 264 modulates the pH dependence of the NAD(+)-dependent D-lactate dehydrogenase, J Biol Chem 267(28) (1992) 20298-20301.

[25] Y. Ishikura, S. Tsuzuki, O. Takahashi, C. Tokuda, R. Nakanishi, T. Shinoda, H. Taguchi, Recognition site for the side chain of 2-ketoacid substrate in D-lactate dehydrogenase, J Biochem 138(6) (2005) 741-749. https://doi.org/10.1093/jb/mvi170.

[26] Y. Zhu, F. Hu, L. Wang, B. Qi, Enhancement of phenyllactic acid biosynthesis by recognition site replacement of D-lactate dehydrogenase from *Lactobacillus pentosus*, Biotechnol Lett 37(6) (2015) 1233-1241. https://doi.org/10.1007/s10529-015-1778-4.

[27] D.A. Benson, M. Cavanaugh, K. Clark, I. Karsch-Mizrachi, D.J. Lipman, J. Ostell, E.W. Sayers, GenBank, Nucleic Acids Res 41(Database issue) (2013) D36-42. https://doi.org/10.1093/nar/gks1195.

[28] E.W. Sayers, T. Barrett, D.A. Benson, E. Bolton, S.H. Bryant, K. Canese, V. Chetvernin, D.M. Church, M. Dicuccio, S. Federhen, M. Feolo, I.M. Fingerman, L.Y. Geer, W. Helmberg, Y. Kapustin, S. Krasnov, D. Landsman, D.J. Lipman, Z. Lu, T.L. Madden, T. Madej, D.R. Maglott, A. Marchler-Bauer, V. Miller, I. Karsch-Mizrachi, J. Ostell, A. Panchenko, L. Phan, K.D. Pruitt, G.D. Schuler, E. Sequeira, S.T. Sherry, M. Shumway, K.

Sirotkin, D. Slotta, A. Souvorov, G. Starchenko, T.A. Tatusova, L. Wagner, Y. Wang, W.J. Wilbur, E. Yaschenko, J. Ye, Database resources of the National Center for Biotechnology Information, Nucleic Acids Res 40(Database issue) (2012) D13-25. https://doi.org/10.1093/nar/gkr1184.

[29] M.M. Bradford, A rapid and sensitive method for the quantitation of microgram quantities of protein utilizing the principle of protein-dye binding, Anal Biochem 72 (1976) 248-254. https://doi.org/0003-2697(76)90527-3.

[30] T. Fujii, M. Shimizu, Y. Doi, T. Fujita, T. Ito, D. Miura, H. Wariishi, N. Takaya, Novel fungal phenylpyruvate reductase belongs to D-isomer-specific 2-hydroxyacid dehydrogenase family, Biochim Biophys Acta 1814(12) (2011) 1669-1676. https://doi.org/10.1016/j.bbapap.2011.05.024.

[31] A.N. Khusnutdinova, R. Flick, A. Popovic, G. Brown, A. Tchigvintsev, B. Nocek, K. Correia, J.C. Joo, R. Mahadevan, A.F. Yakunin, Exploring bacterial carboxylate reductases for the reduction of bifunctional carboxylic acids, Biotechnol J 12(11) (2017). https://doi.org/10.1002/biot.201600751.

[32] S. Kumar, G. Stecher, M. Li, C. Knyaz, K. Tamura, MEGA X: Molecular Evolutionary Genetics Analysis across Computing Platforms, Mol Biol Evol 35(6) (2018) 1547-1549. https://doi.org/10.1093/molbev/msy096.

[33] W. Li, A. Cowley, M. Uludag, T. Gur, H. McWilliam, S. Squizzato, Y.M. Park, N. Buso, R. Lopez, The EMBL-EBI bioinformatics web and programmatic tools framework, Nucleic Acids Res 43(W1) (2015) W580-584. https://doi.org/10.1093/nar/gkv279.

[34] S.F. Altschul, T.L. Madden, A.A. Schaffer, J. Zhang, Z. Zhang, W. Miller, D.J. Lipman, Gapped BLAST and PSI-BLAST: a new generation of protein database search programs, Nucleic Acids Res 25(17) (1997) 3389-3402. https://doi.org/10.1093/nar/25.17.3389.

[35] H.M. Berman, J. Westbrook, Z. Feng, G. Gilliland, T.N. Bhat, H. Weissig, I.N. Shindyalov, P.E. Bourne, The Protein Data Bank, Nucleic Acids Res 28(1) (2000) 235-242.

[36] S.W. Jung, K. Lee, A.E. Cho, Computational approaches to predict binding interactions between mammalian tyrosinases and (S)-(+)-decursin and its analogues as potent inhibitors, RSC Advances 6(52) (2016) 46765-46774. https://doi.org/10.1039/c6ra09365e.

[37] S.C. Lovell, I.W. Davis, W.B. Arendall, 3rd, P.I. de Bakker, J.M. Word, M.G. Prisant, J.S. Richardson, D.C. Richardson, Structure validation by Calpha geometry: phi,psi and Cbeta deviation, Proteins 50(3) (2003) 437-450. https://doi.org/10.1002/prot.10286.

[38] R.A. Friesner, J.L. Banks, R.B. Murphy, T.A. Halgren, J.J. Klicic, D.T. Mainz, M.P. Repasky, E.H. Knoll, M. Shelley, J.K. Perry, D.E. Shaw, P. Francis, P.S. Shenkin, Glide: a new approach for rapid, accurate docking and scoring. 1. Method and assessment of docking accuracy, J Med Chem 47(7) (2004) 1739-1749. https://doi.org/10.1021/jm0306430.

[39] T.A. Halgren, R.B. Murphy, R.A. Friesner, H.S. Beard, L.L. Frye, W.T. Pollard, J.L. Banks, Glide: a new approach for rapid, accurate docking and scoring. 2. Enrichment factors in database screening, J Med Chem 47(7) (2004) 1750-1759. https://doi.org/10.1021/jm030644s.

[40] Schrödinger, LigPrep Release 2018-2, Schrödinger, LLC, New York, NY (2018).

[41] L. Zhu, X. Xu, L. Wang, H. Dong, B. Yu, Y. Ma, NADP+-Preferring D-Lactate Dehydrogenase from *Sporolactobacillus inulinus*, Appl Environ Microbiol 81(18) (2015) 6294-6301. https://doi.org/10.1128/AEM.01871-15.

[42] C. Tokuda, Y. Ishikura, M. Shigematsu, H. Mutoh, S. Tsuzuki, Y. Nakahira, Y. Tamura, T. Shinoda, K. Arai, O. Takahashi, H. Taguchi, Conversion of *Lactobacillus pentosus* D-lactate dehydrogenase to a D-hydroxyisocaproate dehydrogenase through a single amino acid replacement, J Bacteriol 185(16) (2003) 5023-5026. https://doi.org/10.1128/JB.185.16.5023-5026.2003.

[43] S. Kochhar, P.E. Hunziker, P. Leong-Morgenthaler, H. Hottinger, Evolutionary relationship of NAD(+)-dependent D-lactate dehydrogenase: comparison of primary structure of 2-hydroxy acid dehydrogenases, Biochem Biophys Res Commun 184(1) (1992) 60-66. https://doi.org/10.1016/0006-291X(92)91157-L.

[44] S. Hammes-Schiffer, Comparison of hydride, hydrogen atom, and proton-coupled electron transfer reactions, Chemphyschem 3(1) (2002) 33-42. https://doi.org/10.1002/1439-7641(20020118)3:1<33::AID-CPHC33>3.0.CO;2-6.

Figure Captions

Fig. 1 Relative specific activities of 2-HADHs on (a) pyruvate and (b) PPA. Specific activities of wcHADH for pyruvate and pcHADH for PPA corresponding to 100 % relative activity were 428 ± 27.4 and 591 ± 35.7 U mg^{-1}, respectively

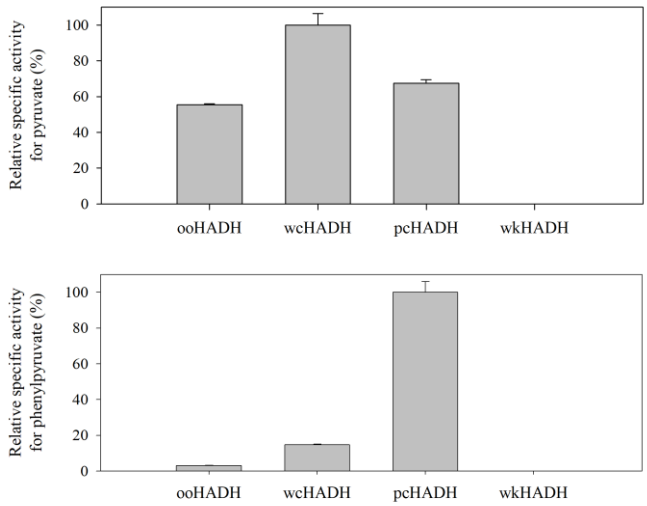

Fig. 2 *In vitro* enzymatic conversion of PPA into PLA by 2-HADHs. Circles, triangles and squares represent conversion by ooHADH, wcHADH and pcHADH, respectively. 100 % concentration corresponds to 20 mM of PLA

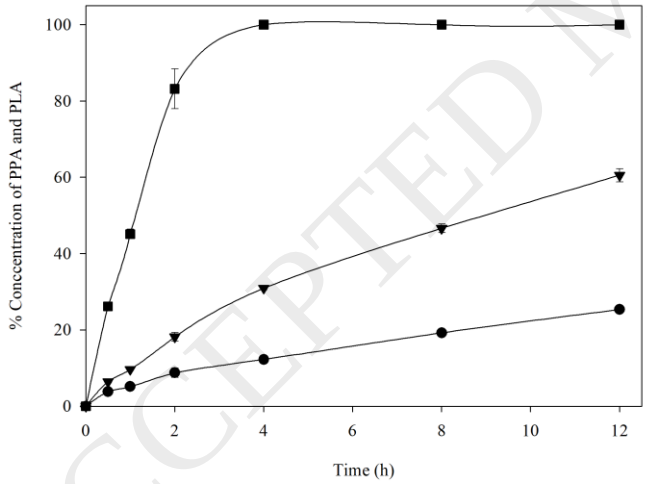

Fig. 3 Phylogenetic analysis presenting (a) unrooted neighbor-joining tree of the 2-HADHs investigated in this study and 365 non-redundant members of D-isomer specific 2-hydroxy acid dehydrogenase family. Proteins are grouped by their characterized functions. GHPR, glyoxylate and hydroxypyruvate reductase; SERA, D-3-phosphoglycerate dehydrogenase; CTBP, C-terminal binding protein; FDH, formate dehydrogenase; D-LDH, D-

lactate dehydrogenase; PDXB, erythronate-4-phosphate dehydrogenase. ⓐ, ⓑ, ⓒ and ⓓ represents oo, wc, pc and wkHADH, respectively. Scale bar indicates 0.5 amino acid substitution per position. (b) unrooted neighbor-joining tree the 2-HADHs investigated in this study and other D-LDHs with known PPA reductase activity. Bootstrap value was >60 %. Accession numbers from the NCBI database are given in brackets. Scale bar indicates 0.2 amino acid substitution per position.

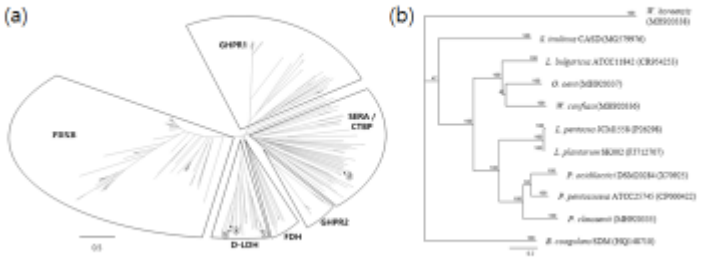

Fig. 4 Sequence alignment of the 2-HADHs and the D-LDHs with PPA activity. Active site residues are shaded in gray, with their residue numbers corresponding to those of pcHADH above.

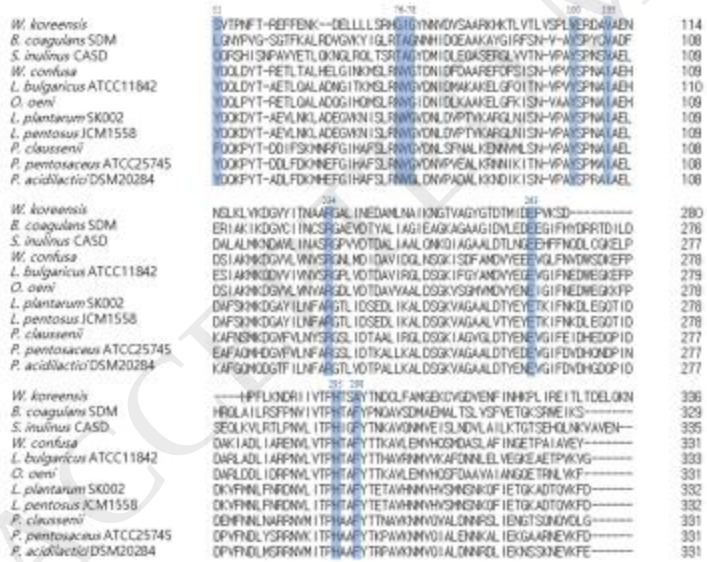

Fig. 5 Relative specific activities of pcHADH wild-type and F51 mutants for PPA. The specific activity of the wild-type corresponding to 100 % relative activity was 525 ± 58.9 U mg^{-1}

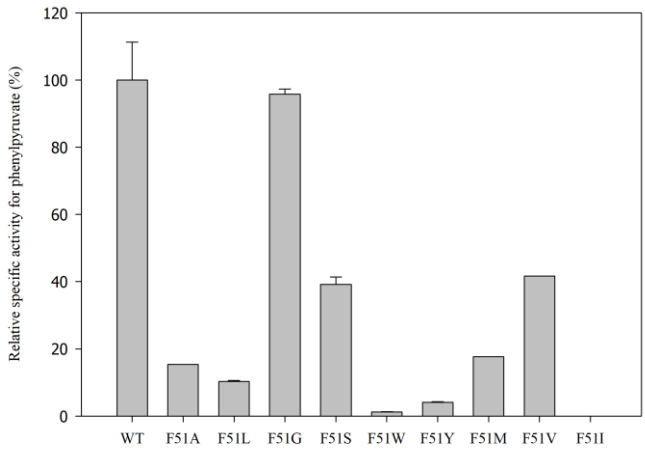

Fig. 6 The active site of the 2-HADHs docked with substrates: (a), ooHADH with pyruvate; (b), ooHADH with PPA; (c), wcHADH with pyruvate; (d), wcHADH with PPA; (e), pcHADH with pyruvate; (f), pcHADH with PPA. The carbon atoms of NADH, substrates docking poses and active site residues are colored in yellow, green and gray, respectively with the residue numbers. The distances are indicated in reference to the Table 3: d1, between NADH and the substrate C_2 atom; d2, between the H295 N_ε atom equivalent and the substrate 2-oxo group; d3, between the centroid of phenyl ring of the F51 (Y52 in oo and wcHADH) and C_3 atom in pyruvate (or the centroid of phenyl group in PPA); d4, between the hydroxyl group of Y52 and substrate C_3 atom in pyruvate (or the centroid of phenyl group in PPA)

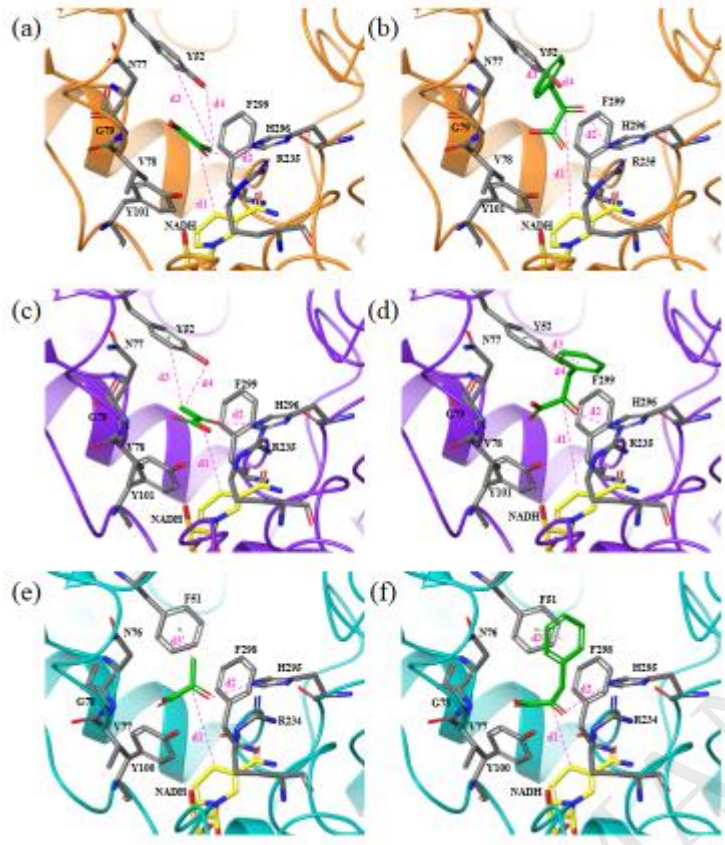

Fig. 7 Comparison of the active site of pcHADH docked with PPA. Wild-type, (a); F51L, (b); F51G, (c); F51S, (d). The distances are indicated in reference to the Table 4: d1, between NADH and the PPA C_2 atom; d2, between the H295 N_ε atom and the substrate 2-oxo group; d3, between the centroid of phenyl group in PPA and the closest heavy atom of the residue 51 side chain; d5, between the carboxylate of PPA and the backbone N of V77; d6, between the carboxylate of PPA and the backbone N of G78.

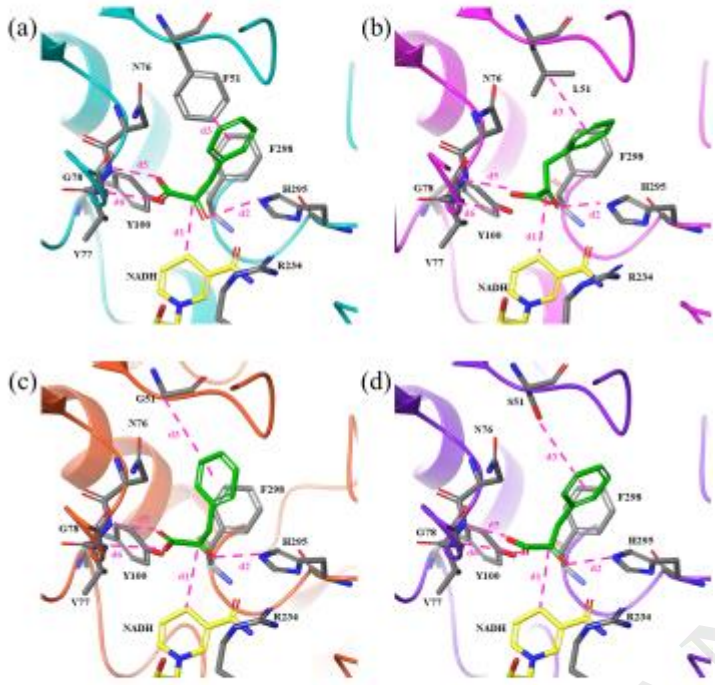

Table 1 Kinetic parameters of 2-HADHs investigated in this study

2-HADH	Kinetic parameters for substrates						$\frac{kcat/Km\ (PPA)}{kcat/Km\ (Pyruvate)} \times 100$ (%)
	Pyruvate			PPA			
	k_{cat} (s^{-1})	K_m (mM)	k_{cat}/K_m ($s^{-1}\ mM^{-1}$)	k_{cat} (s^{-1})	K_m (mM)	k_{cat}/K_m ($s^{-1}\ mM^{-1}$)	
ooHADH	674 ± 22	1.12 ± 0.04	602 ± 1.43	77.8 ± 5.36	15.6 ± 0.53	5.00 ± 0.18	0.83
wcHADH	1434 ± 240	1.28 ± 0.24	1124 ± 23.6	457 ± 15.1	20.3 ± 0.60	22.5 ± 0.07	2.00
pcHADH	459 ± 30	0.56 ± 0.01	813 ± 46.1	472 ± 33.8	0.35 ± 0.05	1348 ± 99.2	165

Table 2 Comparative analysis of activity of wild-type 2-HADHs and D-LDHs reported in the literatures

Bacterial origin of enzymes	Pyruvate				PPA			$\frac{kcat/Km\ (PPA)}{kcat/Km\ (Pyruvate)} \times 100$ (%)	Reference
	k_{cat} (s^{-1})	K_m (mM)	k_{cat}/K_m ($s^{-1}\ mM^{-1}$)		k_{cat} (s^{-1})	K_m (mM)	k_{cat}/K_m ($s^{-1}\ mM^{-1}$)		

L. bulgaricus ATCC11842	NR	NR	NR		11.3	11.4	1.00	-	[4]
P. pentosaceus ATCC25745	320	0.49	658		173	1.73	100	15.2	[9]
S. inulinus CASD	8.85	3.40	22.60		4.94	3.32	1.49	6.59	[13]
P. acidilactici DSM20284	287	0.09	3157		305	2.92	105	3.33	[14]
L. plantarum SK002	NR	0.06	NR		NR	5.40	NR	-	[15]
B. coagulans SDM	23.6	2.20	11		16.5	4.40	3.90	35.5	[16]
L. fermentum JN248	NR	NR	NR		123	1.68	73.0	-	[17]
Lactobacillus sp. CGMCC 9967	NR	NR	NR		47.3	0.82	57.7	-	[18]
W. fluorescens TK1	NR	NR	NR		150	0.40	380	-	[29]
L. pentosus JCM1558	321	0.12	2675		40	0.80	50.0	1.87	[41]

NR: Not reported

Table 3 Binding free energy and the key distances in the modeling of the substrate in 2-HADHs

Enzyme	Pyruvate						PPA				
	$\Delta G_{binding}$ (kcal mol^{-1})	d1 (Å)	d2 (Å)	d3 (Å)	d4 (Å)		$\Delta G_{binding}$ (kcal mol^{-1})	d1 (Å)	d2 (Å)	d3 (Å)	d4 (Å)
ooHADH	-3.32	4.4	2.9	6.9	4.8		-5.31	6.3	3.2	7.4	7.0.
wcHADH	-3.39	4.6	2.9	4.8	3.5		-5.09	5.7	2.7	7.4	6.1
pcHADH	-3.45	5.1	2.8	4.6	N/A		-6.53	4.1	3.3	4.2	N/A

*N/A: Not applicable

$\Delta G_{binding}$, binding free energy; d1, between NADH and the substrate C_2 atom; d2, between the H295 $N\varepsilon$ atom equivalent and the substrate 2-oxo group; d3, between the centroid of phenyl ring of the F51 (Y52 in oo and wcHADH) and C_3 atom in pyruvate (or the centroid of phenyl group in PPA); d4, between the hydroxyl group of Y52 and substrate C_3 atom in pyruvate (or the centroid of phenyl group in PPA)

Table 4 Binding free energy and the key distances in the modeling of PPA in pcHADH wild-type and F51L mutant

pcHADH	$\Delta G_{binding\ (PPA)}$ (kcal mol^{-1})	d1 (Å)	d2 (Å)	d3 (Å)	d5 (Å)	d6 (Å)
Wild type	-6.53	4.1	3.3	3.4	2.8	3.2
F51L	-6.08	4.6	2.8	4.2	2.8	4.8
F51G	-6.36	4.4	2.8	5.4	2.8	3.4
F51S	-6.19	4.2	2.7	5.3	2.6	3.6

$\Delta G_{binding}$, binding free energy; d1, between NADH and the substrate C_2 atom; d2, between the H295 $N\varepsilon$ atom and the substrate 2-oxo group; d3, between the centroid of phenyl group in PPA and the closest heavy atom of the residue 51 side chain; d5, between the carboxylate of PPA and the backbone N of V77; d6, between the carboxylate of PPA and the backbone N of G78